Nickel-Dependent Oligomerization of the Alpha Subunit of Acetyl-Coenzyme A Synthase/Carbon Monoxide Dehydrogenase†

Xiangshi Tan,‡,§ Ioannis Kagiampakis,‖ Ivan V. Surovtsev,‡ Borries Demeler,⊥ and Paul A. Lindahl*,‡,‖

Department of Chemistry, Texas A&M University, College Station, Texas 77843, Department of Biochemistry and Biophysics, Texas A&M University, College Station, Texas 77843, and Department of Biochemistry, University of Texas, Health Science Center, San Antonio, Texas 78229

Received July 24, 2007

ABSTRACT: After activation with $NiCl_2$, the recombinant α subunit of the Ni-containing $\alpha_2\beta_2$ acetyl-CoA synthase/carbon monoxide dehydrogenase (ACS/CODH) catalyzes the synthesis of acetyl-CoA from CO, CoA, and a methyl group donated from the corrinoid-iron-sulfur protein (CoFeSP). The α subunit has two conformations (open and closed), and contains a novel $[Fe_4S_4]$-$[Ni_p\ Ni_d]$ active site in which the proximal Ni_p ion is labile. Prior to Ni activation, recombinant apo-α contain only an Fe_4S_4 cluster. Ni-activated α subunits exhibit catalytic, spectroscopic and heterogeneity properties typical of α subunits contained in ACS/CODH. Evidence presented here indicates that apo-α is a monomer whereas Ni-treated α oligomerizes, forming dimers and higher molecular weight species including tetramers. No oligomerization occurred when apo-α was treated with Cu(II), Zn(II), or Co(II) ions, but oligomerization occurred when apo-α was treated with Pt(II) and Pd(II) ions. The dimer accepted only 0.5 methyl group/α and exhibited, upon treatment with CO and under reducing conditions, the NiFeC EPR signal quantifying to 0.4 spin/α. Dimers appear to consist of two types of α subunits, including one responsible for catalytic activity and one that provides a structural scaffold. Higher molecular weight species may be similarly constituted. It is concluded that Ni binding to the A-cluster induces a conformational change in the α subunit, possibly to the open conformation, that promotes oligomerization. These interrelated events demonstrate previously unrealized connections between (a) the conformation of the α subunit; (b) the metal which occupies the proximal/distal sites of the A-cluster; and (c) catalytic activity.

The nickel-containing {acetyl-coenzyme A synthase; acetyl-coenzyme A decarbonylase/synthase; carbon monoxide dehydrogenase} family of enzymes are found in anaerobic bacteria and archaea that can grow chemoautotrophically using CO_2 or CO as a carbon source (*1*). These enzymes play a major role in the global carbon (CO_2/CO) cycle and they degrade the environmental pollutant TNT (trinitrotoluene). Enzymes from this family are found in the pathogenic bacterium *Clostridium difficile* (*1*, *2*). One class of such enzymes catalyzes both the reversible reduction of CO_2 to CO, reaction [1],

$$CO_2 + 2H^+ + 2e^- \rightleftarrows CO + H_2O \qquad [1]$$

and the synthesis of acetyl-CoA, reaction [2].

$$CH_3\text{-}Co^{3+}FeSP + CO + CoA \rightleftarrows CH_3C(O)\text{-}CoA + Co^{1+}FeSP \qquad [2]$$

CH_3-Co^{3+}FeSP and Co^{1+}FeSP in [2] represent methylated and unmethylated/reduced forms, respectively, of the corrinoid-iron-sulfur protein. This 89 kDa $\alpha\beta$ heterodimer serves as the sole methyl group donor for the reaction.

The most extensively studied enzyme of this class, from the homoacetogen *Moorella thermoacetica*, is a 310 kDa linear $\alpha\beta\beta\alpha$ tetramer which we shall abbreviate *ACS/CODH*[1] (for reviews see refs *3*−*9*). The α and β subunits function largely independently of each other, with β subunits catalyzing reaction [1] and α subunits catalyzing reaction [2]. An extensive proteinaceous tunnel allows CO to migrate from the active-site cluster where it is synthesized in the β subunit

† This work was supported by the National Institutes of Health (GM46441 to P.A.L.), the Robert J. Kleberg Jr. and Helen C. Kleberg Foundation (B.D.), NIH 1 R01 RR022200-01A1 (B.D.), NSF TG-MCB070038 (B.D.), NCI Grant P30 CA054174 (CAUMA), and UTHSCSA ERC (CAUMA).

* To whom correspondence should be addressed. Phone: (979) 845-0956. Fax: (979) 845-4719. E-mail: Lindahl@mail.chem.tamu.edu.

‡ Department of Chemistry, Texas A&M University.

§ Current address: Department of Chemistry, Institute of Biomedical Sciences, Fudan University, Shanghai, 200043, P.R. China.

‖ Department of Biochemistry and Biophysics, Texas A&M University.

⊥ University of Texas.

[1] Abbreviations: ACS, acetyl-coenzyme A synthase; CODH, carbon monoxide dehydrogenase; ACS/CODH, the bifunctional enzyme from *Moorella thermoacetica*; CoFeSP, corrinoid-iron-sulfur protein; CH_3-Co^{3+}FeSP and Co^{1+}FeSP, methylated and reduced forms of CoFeSP, respectively; Ni_p, Ni of the A-cluster located proximal to the Fe_4S_4 cluster; Ni_d, Ni of the A-cluster located distal to the Fe_4S_4 cluster; apo-α, the inactive α subunit of ACS/CODH, obtained prior to activating with $NiCl_2$, which contains the Fe_4S_4 cluster but lacks the Ni ions; $A_{red-act}$, the reductively activated state of the A-cluster obtained upon incubating the activated α subunit in a low-potential reductant; A_{red}-CO, the form of the A-cluster obtained upon incubating $A_{red-act}$ in CO; NiFeC, the EPR signal exhibited by A_{red}-CO; WT, wild-type; CH_3-THF, methyltetrahydrofolate; EPR, electron paramagnetic resonance.

10.1021/bi7014663 CCC: $37.00
Published on Web 09/22/2007

to the active-site in the α subunit, located ~70 Å away, where CO is a substrate in the synthesis of acetyl-CoA. Delivery of CO is regulated by the conformation of the α subunit (see below).

The active-site for reaction [2] is known as the *A-cluster*. It consists of an Fe_4S_4 cubane bridged through a cysteine sulfur to a dinickel subsite consisting of proximal Ni_p and distal Ni_d (*10*). Two other cysteine sulfurs bridge Ni_p and Ni_d. Ni_d is also coordinated by amide nitrogen donors, affording an N_2S_2 square-planar geometry. Ni_p appears to be the site to which CO and methyl groups bind during catalysis, while Ni_d appears to remain in the low-spin 2+ oxidation state in all known redox states of the A-cluster. The A-cluster is reductively activated for catalysis, forming the $A_{red-act}$ state. Although not established, Ni_p may be zerovalent in this state (*4*).

The genes encoding the α and *β* subunits of ACS/CODH have been cloned and overexpressed in *Escherichia coli* (*10*). Once activated with Ni and treated with a low-potential reductant, recombinant ACS/CODH becomes catalytically active. The gene encoding α has been similarly cloned and overexpressed separately, affording the so-called *apo*-α subunit which contains the Fe_4S_4 cubane portion of the A-cluster but not the [Ni_p Ni_d] subsite. Upon activation with Ni, isolated reduced α subunits exhibit ACS catalytic activity (reaction [2]) and the standard EPR and Mössbauer spectroscopic features of the A-cluster. This indicates that the [Ni_p Ni_d] subsite forms upon Ni exposure (*12*−*15*).

Substantial evidence indicates that both isolated α subunits and ACS/CODH are heterogeneous, with at least two forms present in solution populations. Historically, the first evidence for this was the low spin quantification observed for the so-called *NiFeC* EPR signal; this signal is obtained by reducing the enzyme in the presence of CO, which affords the $S = 1/2$ state called A_{red-CO} (*16*−*18*). In WT ACS/CODH, the NiFeC signal quantifies to only 0.1−0.3 spin/α*β*. This range of values suggests that only 10%−30% of α subunits actually exhibit this signal. Insight into why this might occur arose from the discovery that the Ni_p of the A-cluster is labile and can be removed by treatment with 1,10-phenanthroline (*19*). Phen-treatment abolishes the NiFeC signal and all catalytic activity. The effect is reversible, such that Ni can be reinserted into the proximal site. However, only ~0.2 equiv/α of Ni can be removed and reinserted, reinforcing the idea that only a portion of A-clusters within a population contain labile Ni_p (*20*). Mössbauer spectroscopy confirmed this by revealing two forms of the α subunit, with one form (representing 30%−40% of subunits) containing A-clusters that can be prepared in either the A_{red}-CO or $A_{red-act}$ states (*14*, *15*) and with the other form unable to achieve those states. Not coincidentally, only 30%−50% of α subunits in a population can accept a methyl group from CH_3-Co^{3+}FeSP (*21*, *15*) and only ~20% of α subunits can bind CoA (*22*). The origin of this heterogeneity is unclear, but unactivated apo-α subunits were also found to be heterogeneous, suggesting that the effect originates *prior* to Ni-activation (*15*).

X-ray crystallography reveals that the α subunit of ACS/CODH can exist in two conformations, referred to as *open* and *closed* (*10*). The α subunit in two of the four reported structures is in the open conformation with Ni in the proximal site (*10*, *23*). In the other two reported structures, the subunit is in the closed conformation, with Zn in the proximal site of one reported structure and with Cu in that site in the other structure (*24*). Darnault et al. speculated that there might be a correlation between the conformation and the geometrical preference of the metal in the proximal site, with metal ions that prefer tetrahedral geometry (e.g., d^{10} Zn^{2+} or Cu^{1+}) enforcing the closed conformation and Ni^{2+} ions enforcing the open conformation (*10*).

There is certainly a relationship between the metal ion occupying the proximal A-cluster site and catalytic activity. Cu ions can replace Ni in the proximal site of resting WT ACS/CODH, and this abolishes catalysis (*25*). Zn ions can also replace Ni_p, but catalytic activity is abolished only when ACS/CODH is engaged in catalysis (*26*). Since Ni_p is surface-exposed in the open conformation and buried in the closed conformation, Zn may replace Ni only when the α subunit is in the open conformation. This result also suggests that α alternates between open and closed conformations during catalysis but is in the closed conformation in resting enzyme.

There is seemingly sufficient and noncontroversial evidence establishing that the isolated α subunit is a monomer. This was shown in a previous analytical ultracentrifugation study reported from this laboratory (*27*) and by a subsequent X-ray diffraction crystal structure of a homologous isolated subunit from *Carboxydothermus hydrogenoformans* (*23*). This structure was a monomer in the open conformation, with Ni in the proximal site. This structure contributes to the view that Ni in this site enforces the open conformation.

We now report evidence that the Ni-bound catalytically active form of the isolated α subunit from *Moorella thermoacetica* is in a heterogeneous oligomeric state that includes dimers and tetramers. Oligomerization occurs exclusively when either Ni, Pt, or Pd is added to apo-α, and it probably reflects a conformational change that occurs only when these metals bind to the proximal site of the A-cluster. This provides additional evidence for a causal connection between the nature of the proximal metal and the resulting conformation of the α subunit. Further characterization of the dimer indicates that it is heterogeneous, with one subunit playing the catalytic role and the other serving as a structural scaffold. This provides additional insight into the heterogeneous nature of the enzyme.

EXPERIMENTAL PROCEDURES

Preparation of Proteins. M. thermoacetica cells and recombinant *E. coli* strain JM109 containing plasmid pL-HK05 were grown and harvested as described (*10*, *12*) except that $NiCl_2$ was *not* added to the growing cells as was done previously. CoFeSP and methyl transferase were purified as described (*29*) from the *M. thermoacetica* crude extract in an Ar-atmosphere glovebox containing <1 ppm of O_2. Sonicated *E. coli* cell extracts containing recombinant apo-α subunits were passed through an Ni-NTA column as described (*10*). Fractions off the NTA column were concentrated and loaded onto a Superdex-200 gel filtration column (Amersham) equilibrated with 50 mM sodium phosphates, pH 8.0. With a flow rate of 1 mL/min, α-containing fractions eluted between 50 and 80 min; these were collected and concentrated by ultrafiltration (Amicon). Protein concentrations were determined as described (*11*). Resulting recom-

binant apo-α was >90% pure, as quantified by imaging Coomassie-Blue- (Bio-Rad) stained SDS−PAGE gels (Alpha Innotech Imager 2000). Portions were thawed as needed, subjected to a 1 × 20 cm column of Sephadex G25 equilibrated in buffer A (50 mM Tris pH 8.0), divided into aliquots, and either used immediately or refrozen in liquid N_2. Ti^{3+}citrate was prepared from $TiCl_3$ (Aldrich) and standardized by titration against $K_3[Fe(CN)_6]$ (*29*). Co^{1+}FeSP was methylated using CH_3-THF (Sigma) as described (*30*).

Pre-steady-state kinetic experiments were performed at 25 °C with an SF-61 DX2 double-mixing stopped-flow instrument (Hi-Tech Limited, U.K.) installed in an Ar-atmosphere glovebox (MJ Braun, Inc.) containing <1 ppm of O_2. Reactions were monitored in PM mode at 390 nm.

Treatment of Apo-α with $NiCl_2$. The apo-α subunit was concentrated to >20 mg/mL in sodium phosphates pH 8.0, and then treated with 5.0 equiv/α of $NiCl_2$. In other experiments, $CuCl_2$, $ZnSO_4$, $CoCl_2$, $(NH_3)_2[PdCl_4]$, and $K_2[PtCl_4]$ (Sigma/Acros) were also used. After 4 h, the solution was passed through a Hi-load 16/60 Superdex 200 gel filtration column equilibrated in 50 mM sodium phosphates pH 8.0 at a flow rate of 1.0 mL/min. The system was calibrated using gel filtration molecular weight markers (MW-GT-1000, Sigma) and by plotting molecular masses vs elution times, as described (*28*).

Metal Analysis and X-band EPR. Protein samples were digested in 1 M HNO_3 (Fisher, Trace Metal Grade) overnight and then analyzed on a Perkin-Elmer Graphite Furnace AAnalyst 700 spectrometer. X-band EPR spectra were recorded at 10 K on a Bruker EMX spectrometer using a Hewlett-Packard 5352B microwave frequency counter, the ER4102 ST cavity, and the Oxford Instruments ESR 900 Cryostat.

Analytical Ultracentrifugation. Sedimentation velocity data were collected on a Beckmann XL-I analytical ultracentrifuge at the Center for Analytical Ultracentrifugation of Macromolecular Assemblies at the University of Texas Health Science Center at San Antonio. The samples were spun at 40,000 rpm and 20 °C using the An-60 Ti rotor and Epon-charcoal filled 2-channel centerpieces. Concentration profiles were measured using UV absorbance at 280 nm. The sample was dissolved in 50 mM Tris (pH 8.0) buffer and the cells were assembled under anaerobic conditions. The initial protein concentrations for activated α were 2.5, 4.8, and 8.3 μM. Diffusion-corrected sedimentation coefficient profiles were determined with the enhanced van Holde−Weischet method (*31*) as implemented in the UltraScan data analysis software (*32*, *33*). Molecular weight and shape distributions were determined with the 2-dimensional spectrum analysis (*34*) and the genetic algorithm analysis (*35*). Confidence intervals were determined with the Monte Carlo analysis (*36*). The partial specific volume of subunit α was estimated based on protein sequence as implemented in UltraScan and found to be 0.740 ccm/g. Hydrodynamic corrections for buffer density and viscosity were made with UltraScan.

RESULTS

We passed a solution of the recombinant apo-α subunit through a calibrated size-exclusion column. The volume required for apo-α to pass through the column (~75 mL, Figure 1A) corresponded to a molecular mass of ~80 kDa, indicating, as expected, that the apo-α subunit is a monomer in solution. A small portion of the sample eluted at ~68 mL, corresponding to a molecular mass of a dimer (see below). Another sample of apo-α was first activated with Ni and then passed through the column. In this case, the Ni-activated α subunit eluted as a broad peak centered at ~65 mL (Figure 1B), which corresponds to a molecular mass of ~168 kDa (again corresponding to a dimer). Although unresolved, the broadness of the peak of Figure 1B suggested that a fraction of the sample was a monomer, and that another fraction was a higher molecular mass species. The latter species eluted at ~57 mL, which corresponds most closely to a tetramer. These experiments show that *Ni-activation induces the oligomerization of* α*, with dimeric and tetrameric forms dominating.*

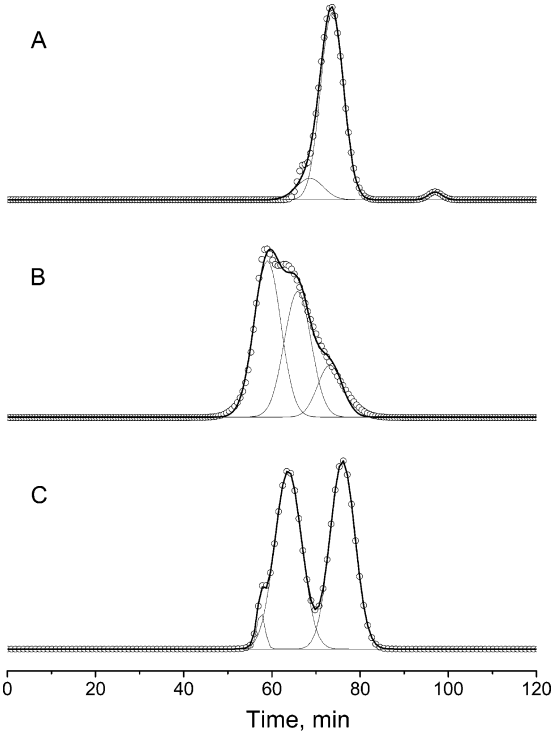

FIGURE 1: Gel filtration chromatography of the α subunit of acetyl-CoA synthase: A, apo-α; B, apo-α after incubation with $NiCl_2$; C, sample from B after concentration and repassage through the column. Thick lines through the data (circles) are composite simulations consisting of the sum of three Gaussian lines (individually shown as thin lines). Best-fit linewidths were determined by fitting the data in C; these linewidths were then fixed while fitting the relative areas under the peaks in A and B. Resolution times were allowed to float slightly for each dataset. The relative percentile areas for the {monomer, dimer, and tetramer} for the simulation in A, B, and C were {88, 12, 0}, {15, 38, 47}, and {48, 49, 3}, respectively. Flow was 1 mL/min such that mL and min units can be interchanged.

Fractions corresponding to the broad peak of Figure 1B were combined, concentrated, and passed a second time through the column. In this case, the population of α subunits eluted mostly as a mixture of monomers and dimers, with a smaller proportion of the tetrameric species (Figure 1C). This suggests that a portion of the oligomers of Figure 1B dissociated into monomers during passage through the size exclusion column, perhaps due to the dissociation of Ni from the enzyme into the elution buffer. Mass action effects resulting from dilution when running through the column may also have contributed to dissociation, which could

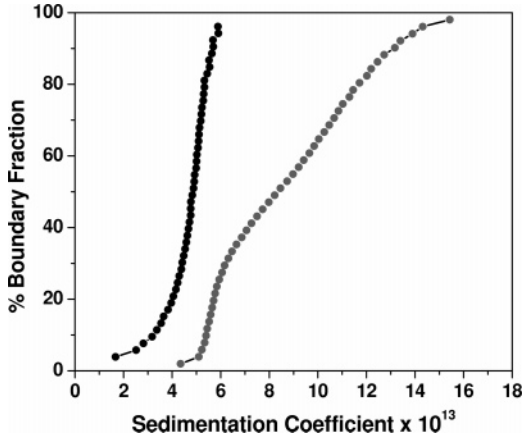

FIGURE 2: Sedimentation velocity results of apo-α (black) and apo-α after Ni has been added (gray). Shown are integral distributions plots of the van Holde−Weischet analysis. While the apo-form appears to be primarily homogeneous with a sedimentation coefficient consistent with a monomer, the increased sedimentation coefficient distributions obtained upon addition of nickel indicate the presence of higher oligomeric forms.

indicate that this process is reversible. In addition, the extent of oligomerization was reduced when low concentrations (<5 mg/mL) of apo-α were used in Ni-activation.

The percentage of the α subunit population in the three oligomeric forms was quantified by fitting the observed peaks with a compilation of three Gaussian functions, one representing each form. The peaks in Figure 1A fit best by assuming that 88% of the α subunit population was present as the monomer and 12% as the dimer. A small amount of the endogenous Ni ions present in cell extracts and/or purification buffers probably associated with apo-α during its isolation to give rise to the dimer. The presence of this small dimeric fraction is consistent with the residual amounts of methyl group transfer activity and EPR spin intensity (see below). The unresolved peak of Figure 1B fit best by assuming 15% monomer, 38% dimer, and 47% tetramer. The peaks of Figure 1C fit best to a model consisting of 48% monomer, 49% dimer, and 3% tetramer. This behavior suggests the following reactions:

$$2\alpha \overset{\text{Ni}}{\rightleftharpoons} \alpha_2$$

$$2\alpha_2 \rightleftharpoons (\alpha_2)_2$$

where the stoichiometry with regard to Ni should not be viewed as specified. Other oligomeric species may also be present. The tetramer is considered to be a dimer of the α_2 dimer.

Sedimentation velocity experiments were performed to further characterize the oligomerization properties of α in its apo form and upon adding Ni to apo-α. The diffusion-corrected sedimentation coefficient distributions derived from the metalated and apo forms of α are shown in Figure 2. Further analysis of the velocity data by genetic algorithm/Monte Carlo analysis suggests that the oligomers are as large as tetramers, consistent with our gel-filtration results. The genetic algorithm−Monte Carlo results, with 95% confidence intervals, indicate the presence of numerous oligomeric species present in the apo-α + Ni sample, including species with molecular weights consistent with monomers, dimers, *trimers*, and tetramers. The presence of trimers was unexpected and difficult to interpret in terms of the pairwise assembly mechanism implied above. Relative proportions of oligomers observed in the apo-α + Ni velocity experiments tended to be variable between repeat experiments, although an increase in oligomerization compared to the nickel-free sample was always observed. Thus, we cannot currently define the oligomeric distribution of Ni-treated α subunits unambiguously. The observed distribution appears to be sensitive to the Ni and protein concentration, and perhaps to other unidentified variables that are currently describable only as batch-to-batch variations.

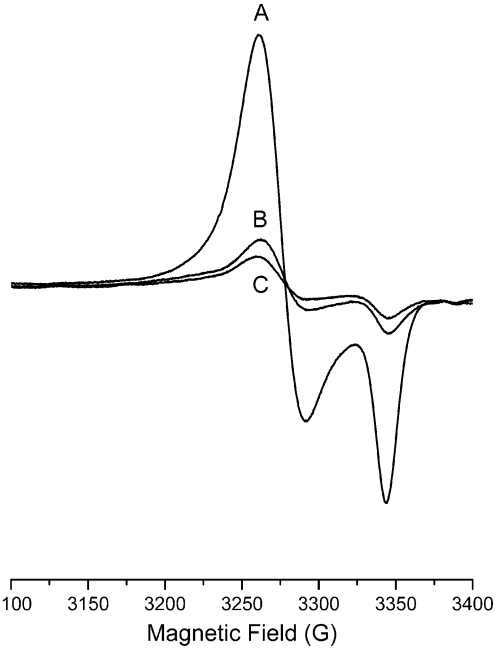

FIGURE 3: Electron paramagnetic resonance of the dimeric form of α (A), apo-α (B), and the dimer-dissociated monomeric form of α (C). Samples were treated with 1 atm of CO and 2 mM dithionite. EPR conditions: temperature, 10 K; microwave power, 20 mW; microwave frequency, 9.48 GHz; modulation amplitude, 11.8 G; sweep time, 328 s; time constant, 20 ms.

Fractions containing the monomer and dimer were collected separately and characterized individually by EPR. We will refer to the monomer form obtained upon dissociation of the dimer as *dimer-dissociated* monomers in contrast to apo-α monomers, allowing for the possibility that these two types of monomers are not identical. When reduced with Ti(III) citrate and exposed to CO, the dimer exhibited the NiFeC EPR signal (Figure 3A), with a spin quantification of 0.4 ± 0.1 spin/α. This might not sound exceptional, but it represents the highest spin concentration ever reported for α from our laboratory. In contrast, similarly treated dimer-dissociated monomers exhibited the NiFeC signal at substantially reduced intensity (0.03 spin/α, Figure 3C). Apo-α exhibited a minor NiFeC signal, with an integrated intensity of 0.03 spin/α (Figure 3B). A similarly prepared ^{57}Fe-enriched dimer sample was examined by Mössbauer spectroscopy. The fraction of A-clusters which exhibited magnetic hyperfine interactions (indicating the A_{red}-CO state) corresponded to ∼40% of the iron in the sample (personal communication, Eckard Münck, Carnegie Mellon University). The details of this study will be published elsewhere.

The Ni and Fe content of apo-α, dimer-dissociated monomers, and dimers was determined. The numbers of (Ni:Fe) ions per α in these forms were {0.3:3.8}, {0.7:3.5}, and

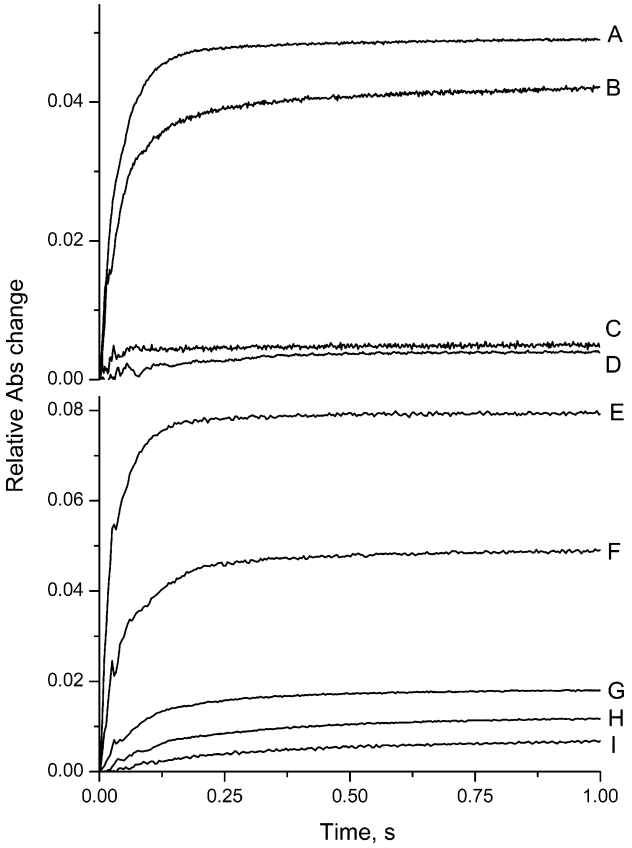

FIGURE 4: Stopped-flow of methyl transfer from methyl corrinoid-iron-sulfur protein (CH_3-Co^{3+}FeSP, 10 μM in all reactions) to the recombinant α subunit. Upper panel: A, dimer (10 μM); B, dimer-dissociated monomers (10 μM), obtained as eluted FPLC fractions of the dimers in A, after overnight incubation in 100 μM $NiCl_2$; C, apo-α (10 μM); D, dimer-dissociated monomer (10 μM). Lower panel: E, F, G, H, and I, dimers with concentrations of 20, 10, 5, 2.5, and 1.5 μM, respectively. All protein concentrations are in terms of monomeric α subunits after mixing. Reactions were monitored at 390 nm, and the buffer was 50 mM TrisHCl, pH 8.0. Ti^{3+}-citrate (1 mM) was present in all of these experiments.

{1.9:4.8}, respectively. These results suggest that apo-α is not identical to dimer-dissociated monomers, in that the latter species contains more Ni. Since the proximal Ni_p ion is labile while Ni_d is not (*19*, *20*), it is reasonable to assume that the loss of Ni_p is responsible for the dissociation of the dimer and that Ni_d remains in dimer-dissociated monomers.

To assess whether dimer-dissociated monomers reassembled into dimers under highly concentrated conditions, we concentrated such monomers and passed them again through the column. In this case, the subunits eluted as monomers. We conclude that dimers dissociate as they pass through the column essentially because Ni dissociates during this passage, not because the α concentration declines below a threshold value required for significant oligomerization.

The ability of the various oligomeric forms of α to accept a methyl group from CH_3-Co^{3+}FeSP was investigated. Both apo-α and dimer-dissociated monomers displayed little activity (Figure 4C and 4D) while the dimer exhibited strong methyl group transfer activity (Figure 4A). The tetrameric form also exhibited methyl group transfer activity at a level comparable to the dimer (data not shown).

Interestingly, the dimer accepted only ~0.5 methyl group per α subunit. When dimer-dissociated monomers were incubated in Ni, the resulting material accepted methyl

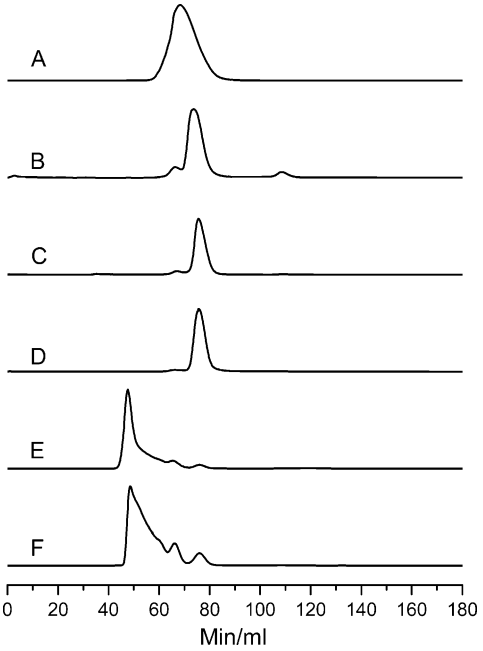

FIGURE 5: Size-exclusion chromatography of metal-ion-treated α subunits (16 mg/mL): A, $NiCl_2$; B, $CuCl_2$; C, $ZnSO_4$; D, $CoCl_2$; E, $(NH_3)_2[PdCl_4]$; F, $K_2[PtCl_4]$.

groups to an extent consistent with the dimer forming (Figure 4B). This reinforces the view that dimerization is Ni-dependent and that dimers, but not monomers, can accept a methyl group from CH_3-Co^{3+}FeSP.

We wondered why the dimer could accept only ~0.5 methyl group/α, and considered the possibility that the amount of methyl group transferred might depend sensitively on the concentration of the α subunit. Accordingly, at some sufficiently low concentration of the α subunit, we hypothesized that the dimer would dissociate, forming monomers that could not accept a methyl group. Perhaps the concentration of α used in the methyl group transfer experiments happened to afford in solution ~50% dimer-dissociated monomers and ~50% dimers (with percentages given in terms of molecular species rather than subunits). If so, the amount of methyl group transferred should increase at higher α concentrations and decrease at lower α concentrations. However, as shown in Figure 4, lower panel, E−I, the amount of methyl group transferred per α subunit was essentially constant at ~0.5 methyl group per α between α concentrations of 1.5−20 μM. We conclude that the explanation just described as to why the α dimer accepts only ~0.5 methyl group per α is incorrect. Rather, these results suggest that in the presence of 5 equiv/α of $NiCl_2$, oligomeric species are fully formed at concentrations as low as 1.5 μM. These results also suggest that *only one subunit of the dimer (and two of the subunits of the tetramer) is inherently able to accept a methyl group*. The EPR and Mössbauer results mentioned above reinforce this conclusion.

Finally, we investigated whether oligomerization is specifically Ni-dependent. We did this by adding Cu^{2+}, Zn^{2+}, Co^{2+}, Pd^{2+}, and Pt^{2+} ions to separate solutions of the apo-α monomer. The addition of Cu^{2+}, Zn^{2+}, and Co^{2+} ions had no influence on the oligomeric state of α; i.e., the monomeric form was uniformly observed (Figure 5B, 5C, and 5D). However, addition of Pd^{2+} and Pt^{2+} resulted in a population of oligomeric states (Figure 5E and 5F) including substantial

```
Alpha:    DKIFEGAIPE GKEPVALFRE VYHGAITATS YA-EILLNQA --
Beta:     DNSRAVDLLM AMANDLGVDT PKVPFV-A-S -APEAMSGKA AA
Common:   D                            A S  A E     A

Alpha:    IRTYGPDH PVGYPDTAYY L--PVIRCFS GEEV-KKLGD LPPI
Beta:     IGTWWVSL --GVP-THVG TMPPVEGSDL IYSILTQIAS DVYG
Common:   I T        G P T       PV

Alpha:    LNRKRA QVSP-VLNFE NARLAGEA-T WYAAEIIE-A LRY-LK
Beta:     GYFIFE MD-PQVAARK ILD-ALEYRT WKLGVHKEVA ERYETK
Common:             P V          A E  T W      E A  RY  K
```

FIGURE 6: Amino acid alignment of the N-terminal domain of the α subunit with a region of the *β* subunit. The α sequence begins at Asp005 and ends at Lys120. The *β* sequence begins at Asp552 and ends at Lys669.

amounts of dimers and higher oligomeric forms, perhaps as large as hexamers. Pt-induced dimer-containing fractions were found to be incapable of accepting a methyl group from CH_3-Co^{3+}FeSP. This experiment suggests that the ability of form oligomers is specific to group 10 divalent metal ions (Ni, Pd, Pt) whereas the ability of such oligomers to exhibit catalytic activity is specific for Ni. One appealing scenario is that the preference for square-planar geometry associated with group 10 metals induces a conformational change in α that favors oligomerization, but that only the presence of Ni in the A-cluster allows catalytic activity.

DISCUSSION

This study originated serendipitously when we discovered that the α subunit of ACS/CODH did not migrate by gel filtration as a single monomeric species, as we had expected. Further examination of this phenomenon revealed that oligomerization was Ni-dependent and was correlated to the development of catalytic activity. There can be little doubt that the added Ni binds to a particular site on the α subunit. Since there are only two sites on α known to bind Ni (the distal and proximal sites of the A-cluster), we limit our consideration to these. There is abundant evidence that Ni ions bound to the proximal site are labile and that those bound at the distal site are not. Thus, we conclude that *oligomerization is induced when a* Ni^{2+} *ion binds to the proximal site of the A-cluster*.

Absent a crystal structure, it is difficult to determine how the binding of Ni to the proximal site might induce oligomerization, but it again seems likely that Ni-binding induces a conformational change in the subunit. As mentioned in the introductory comments, a structural correlation between the nature of the metal occupying the proximal site and the conformation of α has already been noted. The two structures of α reported with Ni in the proximal site are both in the open conformation, while the two structures reported with Cu or Zn in the proximal site are in the closed conformation (*10*, *23*, *24*). Darnault et al. hypothesized that metal ions which favor tetrahedral geometry (Zn^{2+} or Cu^{1+}) enforce the closed conformation (*10*).

Since the Ni_p site in the open conformation involves three endogenous cysteinates in a planar environment about the Ni, we propose that *metal ions in oxidation states which prefer planar geometry (e.g.,* Ni^{2+}*) enforce the open conformation* and that it is this conformational change which promotes oligomerization. This proposal is supported by the oligomerization caused by the addition of Pd^{2+} and Pt^{2+} ions to solutions of apo-α. Pd^{2+} and Pt^{2+} are both d^8 transition metal ions that have a strong preference for square-planar geometry. Readers should be aware that we have not shown directly that either Pd or Pt binds at the proximal A-cluster site.

Another important issue is whether Ni-dependent oligomerization and/or conformational change is/are functionally relevant. Since we cannot obtain monomers with a full complement of Ni in the A-cluster, we cannot know whether oligomerization is an *inherent* requirement for activity, or a simple consequence of some other property which is inherently required for activity (e.g., the presence of Ni in the A-cluster or the open conformation). Given that multiple oligomeric states form and that α is "designed" to be associated with the *β* subunit as an α*ββ*α tetramer (with no α:α interactions) we find it unlikely that oligomerization is directly functionally relevant. Thus, we view oligomerization simply as a *reporter* of the conformational change promoted by Ni-binding.

It seems more likely that Ni^{2+} binding at the proximal A-cluster site enforces the open conformation of the α subunit and that this is relevant to the catalytic mechanism of the enzyme. Moreover, the apparent correlation between the *planar geometrical preference* of Ni^{2+} ions with the open conformation of α suggests a mechanism by which the conformation of α could be altered during catalysis, namely, by the geometrical preferences associated with the oxidation state of Ni_p. However, further studies will be required to examine this proposal further.

Functional α *Dimers Are Heterogeneous.* Our results indicate that the dimeric form of α is heterogeneous and contain two types of subunits, to be referred to as *catalytic* and *structural* subunits, where A-clusters in catalytic subunits can accept a methyl group while those in structural subunits cannot. Moreover, the A-cluster in catalytic subunits can be reduced and bound with CO to afford the A_{red}-CO state and exhibit the NiFeC EPR signal while that in structural subunits cannot access this redox state. The tetrameric form of alpha can be similarly constituted (as a dimer of heterogeneous dimers), whereas the putative trimeric form could not be understood in this way.

We recently found that populations of apo-α subunits (monomers) were heterogeneous according to Mössbauer spectroscopy, with ~30% in the active form and 70% in the inactive form (*15*). Equivalent spectra were observed for Ni-activated α subunits, which now are shown to be mixtures of monomeric, dimeric, (perhaps trimeric), and tetrameric

forms. These results suggested that the heterogeneity of the α subunits arises *before* Ni-activation and oligomerization. Assuming this, there should be an ample supply of both active and inactive subunits ready to oligomerize once Ni has been added. Additional studies will be required to clarify the range of observed variability as well as the source of that variability. In principle, it would seem that nascent α subunits dissociating from a ribosome *must* be homogeneous, suggesting that the observed heterogeneity is introduced after translation but before Ni-activation. This is an intriguing issue that will require further study.

The ability of α to dimerize can be rationalized in terms of the ability of α to interact with the *β* subunit of ACS/CODH. Doukov et al. (*24*) reported that the N-terminal domain of the α subunit has a similar Rossmann fold to the domain in the *β* subunit to which the α subunit interacts, and they suggested that the two domains might be related by a gene duplication event. Although the percent identity in the interacting region is low (Figure 6), it contributes to the noted relatedness of the two tertiary structures. Given the results presented here, it also suggests that the structural α subunit of the dimer may serve as surrogate for the interacting *β* subunit domain of native ACS/CODH.

Comparison to Previous Results. We were surprised to discover that the catalytically active form of α is a dimer and other oligomers, rather than a monomer, because previous reports had indicated that α was a monomer. However, the α subunits used by Xia et al. (*27*) in their analytical ultracentrifugation experiments were *inactive*, which is consistent with our current results. The only caveat here is that the inactivity observed in those previous samples likely arose for reasons besides the lack of Ni, since no activity developed even after adding Ni ions.

More difficult to reconcile is the monomeric X-ray crystal structure obtained for the homologous subunit from *Carboxydothermus hydrogenoformans* (*23*). Their results reveal a catalytically active monomer in the open conformation with both Ni_p and Ni_d present in the A-cluster. One possibility that would reconcile their results with those reported here is that, unlike the α subunit from *M. thermoacetica*, the corresponding monomer from *C. hydrogenoformans* may not have the appropriate subunit:subunit contacts in the open conformation to promote oligomerization even though the subunit undergoes the same Ni-dependent (and mechanistically important) conformational change. Curiously, the reported NiFeC spin intensity for their samples corresponded to 0.14 spin/α, a value which implies a similar type and degree of heterogeneity as that observed in our samples, yet there is no structural evidence of heterogeneity. Further studies will be required to settle these and other issues which are critical to understanding the catalytic mechanism of this unusual and intriguing enzyme.

ACKNOWLEDGMENT

We thank Eckard Münck and Audria Stubna for collecting Mössbauer spectra of the α dimer, Frank Raushel and Dao Feng Xiang for assistance in preliminary FPLC studies, Patti LiWang for allowing one of the authors (I.K.) to participate in this study, and David E. Graham for helpful discussion regarding sequence alignments.

REFERENCES

1. Lindahl, P. A., and Graham D. E. (2007) Acetyl-Coenzyme A synthases and Nickel-containing carbon monoxide dehydrogenases, in Vol. 2 of *Metal Ions in Life Sciences* (Sigel, A., Sigel, H., and Sigel, R. K. O., Eds.) pp 357−416, John Wiley & Sons, Ltd., Chichester, U.K.
2. Shouqin Huang, S., Lindahl, P. A., Wang, C., Bennett, G. N., Rudolf, F. B., and Hughes, J. B. (2000) 2,4,6-Trinitrotoluene (TNT) Reduction by Carbon Monoxide Dehydrogenase from *Clostridium thermoaceticum*, *Appl. Environ. Microbiol. 66*, 1474−1478.
3. Drennan, C. L., Doukov, T. I., and Ragsdale, S. W. (2004) The metalloclusters of carbon monoxide dehydrogenase/acetyl-CoA synthase: a story in pictures, *J. Biol. Inorg. Chem. 9*, 511−515.
4. Lindahl, P. A. (2004) Acetyl-Coenzyme A Synthase: The Case for a Ni_p^0-Based Mechanism of Catalysis, *J. Biol. Inorg. Chem. 9*, 516−524.
5. Volbeda, A., and Fontecilla-Camps, J. C. (2004) Crystallographic evidence for a CO/CO_2 tunnel gating mechanism in the bifunctional carbon monoxide dehydrogenase/acetyl coenzyme A synthase from *Moorella thermoacetica*, *J. Biol. Inorg. Chem. 9*, 525−532.
6. Brunold, T. C. (2004) Spectroscopic and computational insights into the geometric and electronic properties of the A-cluster of acetyl-coenzyme A synthase, *J. Biol. Inorg. Chem. 9*, 533−541.
7. Riordan, C. G. (2004) Synthetic chemistry and chemical precedents for understanding the structure and function of acetyl coenzyme A synthase, *J. Biol. Inorg. Chem. 9*, 542−549.
8. Ragsdale, S. W. (2004) Life with carbon monoxide, *Crit. Rev. Biochem. Mol. Biol. 39*, 165−195.
9. Hegg, E. L. (2004) Unraveling the structure and mechanism of acetyl-coenzyme A synthase, *Accounts Chem. Res. 37*, 775−783.
10. Darnault, C., Volbeda, A., Kim, E. J., Legrand, P., Vernede, X., Lindahl, P. A., and Fontecilla-Camps, J. C. (2003) Ni-Zn-[Fe4S4] and Ni-Ni-[Fe4S4] Clusters in Closed and Open Subunits of Acetyl-CoA Synthase/Carbon Monoxide Dehydrogenase, *Nat. Struct. Biol. 10*, 271−279.
11. Loke, H.-K., Bennett, G., and Lindahl, P. A. (2000) Active Acetyl-CoA Synthase from *Clostridium thermoaceticum* obtained by Cloning and Heterologous Expression of acsAB in *Escherichia coli*, *Proc. Natl. Acad. Sci. U.S.A. 97*, 12530−12535.
12. Loke, H. K., Tan, X., and Lindahl, P. A. (2002) Genetic construction of truncated and chimeric metalloproteins derived from the α subunit of acetyl-CoA synthase from *Clostridium thermoaceticum*, *J. Am. Chem. Soc. 124*, 8667−8672.
13. Xia, J., and Lindahl, P. A. (1996) Assembly of an Exchange-Coupled [Ni : Fe4S4] Cluster in the α Metallosubunit of CO Dehydrogenase from *Clostridium thermoaceticum* with Spectroscopic Properties and CO-Binding Ability Mimicking the Acetyl-CoA Synthase Active Site, *J. Am. Chem. Soc. 118*, 483−484.
14. Xia, J., Hu, J., Popescu, C., Lindahl, P. A., and Münck, E. (1997) Mössbauer and EPR Study of the Ni-Activated α Subunit of Carbon Monoxide Dehydrogenase from *Clostridium thermoaceticum*, *J. Am. Chem. Soc. 119*, 8301−8312.
15. Bramlett, M. R., Stubna, A., Tan, X., Surovtsev, I. V., Münck, E., and Lindahl, P. A. (2006) Mössbauer and EPR Study of Recombinant Acetyl-CoA Synthase from *Moorella thermoacetica*, *Biochemistry*, *45*, 8674−8685.
16. Lindahl, P. A., Münck, E., and Ragsdale, S. W. (1990) CO Dehydrogenase from *Clostridium thermoaceticum*; EPR and Electrochemical Studies in CO2 and Argon Atmospheres, *J. Biol. Chem. 265*, 3873−3879.
17. Lindahl, P. A., Ragsdale, S. W., and Münck, E. (1990) Mössbauer Study of CO Dehydrogenase from *Clostridium thermoaceticum*, *J. Biol. Chem. 265*, 3880−3888.
18. Shin, W., and Lindahl, P. A. (1993) Low spin quantitation of NiFeC EPR signal intensity from carbon monoxide dehydrogenase is not due to damage incurred during protein purification, *Biochem. Biophys. Acta 1161*, 317−322.
19. Shin, W., and Lindahl, P. A. (1992) Discovery of a Labile Nickel Ion Required for CO/Acetyl-CoA Exchange Activity in the NiFe Complex of Carbon Monoxide Dehydrogenase from *Clostridium thermoaceticum*, *J. Am. Chem. Soc. 114*, 9718−9719.
20. Shin, W., Anderson, M. E., and Lindahl, P. A. (1993) Heterogeneous Nickel Environments in Carbon Monoxide Dehydrogenase from *Clostridium thermoaceticum*, *J. Am. Chem. Soc. 115*, 5522−5526.

21. Barondeau, D. P., and Lindahl, P. A. (1997) Methylation of Carbon Monoxide Dehydrogenase from Clostridium thermoaceticum and Mechanism of Acetyl Coenzyme A Synthesis, *J. Am. Chem. Soc. 119*, 3959−3970.
22. Wilson, B. E., and Lindahl, P. A. (1999) Equilibrium Dialysis Study and Mechanistic Implications of Coenzyme A Binding to Acetyl-CoA Synthase/Carbon Monoxide Dehydrogenase from *Clostridium thermoaceticum*, *J. Biol. Inorg. Chem.* **1999**, *4*, 742−748.
23. Svetlitchnyi V, Dobbek, H., Meyer-Klaucke, W., Meins, T., Thiele, B., Romer, P., Huber, R., and Meyer, O. (2004) A functional Ni-Ni-[4Fe-4S] cluster in the monomeric acetyl-CoA synthase from *Carboxydothermus hydrogenoformans*, *Proc. Natl. Acad. Science U.S.A. 101*, 446−451.
24. Doukov, T. I., Iverson, T. M., Seravalli, J., Ragsdale, S. W., and Drennan, C. L. (2002) A Ni-Fe-Cu center in a bifunctional carbon monoxide dehydrogenase/acetyl-CoA synthase, *Science 298*, 567−572.
25. Bramlett, M. R., Tan, X., and Lindahl, P. A. (2003) Inactivation of Acetyl-CoA Synthase/Carbon Monoxide Dehydrogenase by Copper, *J. Am. Chem. Soc. 125*, 9316−9317.
26. Tan, X., Bramlett, MR., and Lindahl, P. A. (2004) Effect of Zn on Acetyl Coenzyme A Synthase: Evidence for a Conformational Change in the α Subunit during Catalysis, *J. Am. Chem. Soc. 126*, 5954−5955.
27. Xia, J., Sinclair, J. F., Baldwin, T. O., and Lindahl, P. A. (1996) CO Dehydrogenase from *Clostridium thermoaceticum*: Quaternary Structure and Stoichiometry of its SDS-Induced Dissociation, *Biochemistry 35*, 1965−1971.
28. Marti-Arbona, R., Xu, C., Steele, S., Weeks, A., Kuty, G. F., Seibert, C. M., and Raushel, F. M. (2006) Annotating enzymes of unknown function: N-formimino-L-glutamate deiminase is a member of the amidohydrolase superfamily, *Biochemistry*, *45*, 1977−2005.
29. Maynard, E. L., Sewell, C., and Lindahl, P. A. (2001) Kinetic Mechanism of Acetyl-CoA Synthase: Steady-State Synthesis at Variable CO/CO_2 Pressures, *J. Am. Chem. Soc. 123*, 4697−4703.
30. Tan, X., Sewell, C., and Lindahl, P. A. (2001) Stopped-flow kinetics of methyl group transfer between the corrinoid-iron-sulfur protein and acetyl-coenzyme A synthase from *clostridium thermoaceticum*, *J. Am. Chem. Soc. 124*, 6277−6284.
31. Demeler, B., and van Holde, K. E. (2004) Sedimentation velocity analysis of highly heterogeneous systems, *Anal. Biochem. 335*, 279−288.
32. Demeler, B. (2005) In *Modern Analytical Ultracentrifugation: Techniques and Methods* (Scott, D. J., Harding, S. E., and Rowe, A. J., Eds.) pp 210−229, Royal Society of Chemistry, U.K.
33. See http://www.ultrascan.uthscsa.edu.
34. Brookes, E., Boppana, R. V., and Demeler, B. (2006) Computing Large Sparse Multivariate Optimization Problems with an Application in Biophysics. SC2006, Tampa, FL, U.S.A. IEEE 0-7695-2700-0/06.
35. Brookes, E., and Demeler, B. (2006) Genetic Algorithm Optimization for obtaining accurate Molecular Weight Distributions from Sedimentation Velocity Experiments. Analytical Ultracentrifugation VIII, *Prog. Colloid Polym. Sci. 131*, 78−82.
36. Demeler, B., and Brookes, E. (2007) Monte Carlo Analysis of Sedimentation Experiments. Progress in Colloid and Polymer Science, in press.

BI7014663